VILNIUS TECH
Vilnius Gediminas Technical University

Proceedings of the 13th International Scientific Conference

ENVIRONMENTAL ENGINEERING

April 23–24, 2026, Vilnius, LITHUANIA

eISSN 2029-7092
eISBN 978-609-476-444-8
Article ID: enviro.2026.2544
https://doi.org/10.3846/enviro.2026.2544

MAPPING URBAN AIR POLLUTION IN DATA-SCARCE AREAS USING GIS AND SATELLITE DATA

Alessandra CHIAPPINI*, Giorgio PASSERINI

Department of Industrial Engineering and Mathematical Sciences, Università Politecnica delle Marche, 60131 Ancona, Italy

Received 13 March 2026; revised 19 March 2026; accepted 20 March 2026

Abstract. Assessing air quality in urban areas is often challenging, especially in areas where ground-based monitoring networks are scarce or even absent. Due to local policies or limited resources, many areas in Italy lack continuous environmental monitoring over time and space.

To overcome this problem, in this study, we offer a practical GIS-based workflow to help make initial air pollution assessments when data is limited. Using the Sorrento Peninsula in Italy as case study, we implement the workflow, using a mix of satellite data and site-specific geolocalized data, to map out where key pollutants like nitrogen dioxide (NO_2) and fine particulate matter ($PM_{2.5}$) are found across the area.

The method brings together data on NO_2 in the lower atmosphere from the Sentinel-5P TROPOMI sensor and $PM_{2.5}$ estimates that come from measuring aerosol optical depth (AOD). We process all this information using QGIS and overlay it with other useful maps, like roads and ferry routes from OpenStreetMap, port locations, land use, and urbanization. By layering these details, we can spot pollution hotspots and better understand how city life and seasonal tourism (strong in the study area), like heavy road traffic or busy ports, influence air quality.

The results show that GIS satellite mapping provides a continuous spatial approximation of air quality, effectively identifying key areas in locations with limited or no in-situ monitoring. This workflow is replicable and can sustain environmental agencies and urban planners with a cost-effective tool for early hotspot detection and urban exposure assessment to inhance policy support and monitoring strategies in Data-sparse environments.

Keywords: air quality mapping, Satellite remote sensing, Data-sparse environments, GIS, replicable workflow, hotspot detection.

1. Introduction

Air pollution remains one of the most significant environmental and public health concerns in urban settings globally (World Health Organization, 2021). Cities have expanded rapidly over recent decades, and the associated rise in road traffic, residential heating, and industrial activity has placed growing pressure on ambient air quality, with direct consequences for both human health and ecosystem functioning. Among the pollutants of greatest concern, nitrogen dioxide (NO_2) and fine particulate matter ($PM_{2.5}$) stand out for their well-established links to respiratory and cardiovascular morbidity a relationship that has driven air pollution control to the top of environmental and health policy agendas internationally (Lelieveld et al., 2015). Against this backdrop, air quality monitoring networks have taken on a role that extends well beyond routine measurement (de Hoogh et al., 2018). The data they generate underpin decisions across a broad range of domains: from land use planning and urban development to the enforcement of regulatory standards set out in European directives, and the design of early warning protocols intended to protect vulnerable populations from acute exposure events (European Environment Agency, 2023). Without accurate and timely observational data, evaluating the effectiveness of remediation policies or characterizing pollutant dispersion dynamics at the local scale becomes effectively intractable. Dense, spatially representative assessment nevertheless remains difficult to achieve, particularly in regions where ground-level measurement networks are sparse or entirely absent. Across numerous areas, several Italian territories being a notable case, structural constraints, elevated maintenance costs, and local governance decisions have resulted in a chronic deficit of continuous spatiotemporal data. This observational fragmentation precludes a comprehensive characterization of pollution phenomena, leaving extensive "blind zones" in which population exposure cannot be adequately quantified.

* Corresponding author. E-mail: *a.chiappini@staff.univpm.it*

In such settings, broadly referred to as data-sparse environments, the integration of Geographic Information Systems (GIS) with satellite remote sensing technologies emerges as both a practical and increasingly indispensable methodological response (Gupta et al., 2006). Satellite-derived products serve as essential proxies, compensating for the spatial gaps inherent to the absence of ground-based monitoring infrastructure (Bechle et al., 2013). Adopting this combined approach enables the transition from discrete point measurements to spatially continuous mapping, facilitating the identification of concentration gradients and pollution hotspots even in analytically challenging environments. The present study accordingly proposes a GIS-based methodological workflow designed to support the preliminary assessment of ambient air quality in data-scarce territories, employing the Sorrento Peninsula as a case study to evaluate the applicability and robustness of the proposed approach.

2. Materials and methods

2.1. Study domain

The area covered by this research is the Sorrento Peninsula (Figure 1), a promontory located in the Campania region (southern Italy) that acts as a natural watershed between the Gulf of Naples and the Gulf of Salerno. From a geophysical standpoint, the territory presents an extremely complex orography, dominated by the Lattari Mountains, whose steep slopes and deep valleys significantly influence local wind regimes and, consequently, the dispersion and accumulation of air pollutants (Giovannini et al., 2020).

Note: The image illustrates the study domain by integrating different levels of detail: on the left, the regional location in Italy and the detail of the peninsula, between the Gulf of Naples and the Gulf of Salerno; on the right, the analysis of the complex topography using Google Terrain layers, highlighting the administrative boundaries obtained from the ISTAT database.

Figure 1. Geospatial framework and morphological characterization of the Sorrento Peninsula

The settlement structure is a polycentric urban system with high population density, comprising several municipalities within the so-called Naples agglomeration, interconnected by a single main road that constitutes the primary corridor for vehicular traffic, frequently subject to critical congestion episodes. The main anthropogenic emission sources are road traffic, port activities (characterized by intense traffic of hydrofoils, ferries, charter boats, recreational vessels, and cruise ships) and residential heating (Murena et al., 2018).

A distinctive feature of the area is the marked seasonal variability of environmental pressures, closely tied to international tourist flows: during summer months, the sharp increase in floating population drives peak emissions from both maritime and road transport (Contini et al., 2011). The combination of complex terrain and heterogeneous pollutant sources makes the Sorrento Peninsula a particularly suitable case study for validating satellite mapping methodologies in contexts where ground-based monitoring networks are discontinuous.

A key factor behind the choice of the Sorrento Peninsula as a case study is the substantial absence of a fixed and widespread air quality monitoring network. The area currently lacks permanent monitoring stations ensuring continuous spatial and temporal coverage. As shown in Figure 2, only two mobile monitoring stations are present (indicated in blue), positioned at strategic locations but with an extremely localized measurement range; the fixed stations belonging to the national network are situated outside the study area entirely. Moreover, the competent authority in charge of the monitoring via the mobile stations confirmed that few campaigns were conducted in the past and the most recent measurements refer to 2018 for just one station, but for only a few months for which no satellite data are available, making it impossible to use it to validation purposes with ground data, in the specific case. Regarding the fixed station, there are no records for NO_2 and $PM_{2.5}$ for the entire 2025.

Note: Location of the two mobile control units, indicated in blue, and of the Environmental Protection Regional Agency from Campania Region (ARPAC) fixed network control units, in black. Overlayed to the complex topography by Google Terrain layers, and the administrative boundaries obtained from the ISTAT database.

Figure 2. Location of the control units

These mobile infrastructures present significant operational limitations for a comprehensive environmental analysis:

– Limited areal coverage: the punctual nature of the sampling does not allow for the reconstruction of

pollutants distribution across the peninsula's entire orographic complexity.
- Temporal discontinuity: the surveys do not occur continuously, preventing the analysis of long-term trends or the identification of sudden peaks linked to specific meteorological or anthropogenic events.
- Data accessibility: the datasets collected by these stations are not directly accessible in real time or via open data portals, as the information is usually released upon specific requests from individual municipalities to the relevant environmental agencies.

This data-scarcity scenario makes the integration of satellite proxies not only a technological opportunity, but a methodological necessity to provide a consistent and distributed knowledge framework across the entire peninsula.

Regarding air quality composition, the complex interaction between landforms and human activities determines a heterogeneous emissions profile for the Sorrento Peninsula. The main identified environmental pressures and their associated pollutants are summarized in Table 1 below.

Road traffic concentrated in narrow arteries and urban hotspots, is responsible for high concentrations of NO_2, PM_{10}, $PM_{2.5}$, and carbon monoxide (CO). At the same time, maritime traffic along tourist routes and in port areas contributes significantly to emissions of NO_2, sulfur oxides (SO_2), and fine particulate matter. Seasonal sources related to residential heating and peaks in tourist attendance, as well as episodic natural sources for PM_{10}, are also involved.

Table 1. Summary of the main environmental pressures and associated pollutants in the study area

Source	Main pollutants	Notes
Road traffic	NO_2, $PM_{2.5}$, PM_{10}, CO	Urban hotspot, narrow streets
Maritime traffic	NO_2, NO_x, SO_2, $PM_{2.5}$, PM_{10}	Port areas and touristic routs
Seasonal tourism	NO_2, $PM_{2.5}$	Summer peaks
Residential heating	$PM_{2.5}$, NO_x	Densely populated areas
Natural sources	PM_{10}	Sporadic

For the purposes of this research the analysis focused primarily on NO_2 and $PM_{2.5}$. This choice is supported by three fundamental criteria:

1. Cross-cutting Relevance: Both pollutants are critical indicators for the impact of both vehicle and maritime traffic, representing the main drivers of health risk in the area (Cohen et al., 2017).

2. Accessibility and Data Continuity: NO_2 is monitored with high precision by the TROPOMI sensor (Copernicus Sentinel-5P, 2021; Veefkind et al., 2012), while $PM_{2.5}$ can be effectively estimated using Aerosol Optical Depth (AOD) data derived from remote sensing (van Donkelaar et al., 2016).

3. Cartographic Effectiveness: These pollutants are ideally suited to continuous spatial mapping in a GIS environment, allowing the production of consistent concentration maps even in the absence of a widespread ground-based network (Guevara et al., 2021).

Although SO_2 represents a specific indicator for port activities, at this stage it was considered a secondary parameter, favoring a pollutant-focused model with greater availability of high-temporal-resolution satellite proxies.

2.2. Workflow architecture

The proposed air quality mapping workflow, shown in Figure 3, follows four sequential phases. The structure reflects a pragmatic constraint: transforming raw satellite data into geospatial outputs usable for urban planning within a limited timeframe.

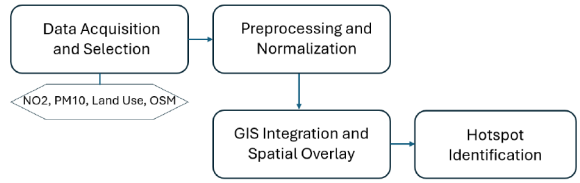

Figure 3. Architecture of the proposed methodological workflow, GIS- and remote sensing-based, for air quality mapping in data-sparse environments

1. Data Acquisition and Selection: Sentinel-5P TROPOMI products for NO_2 and MODIS/AOD data for $PM_{2.5}$ estimation are downloaded as primary inputs (Sorek-Hamer et al., 2020). Land use information is sourced from the 2018 Corine dataset at 100 m resolution, accessed through the Copernicus service. Road network, port, and ferry route geometries are extracted from OpenStreetMap (OSM) directly within the GIS environment — these vector layers are indispensable for attributing measured concentrations to specific emission sources.
2. Preprocessing and Normalization: NetCDF products are converted to 32-bit float TIFF format. This is not a trivial choice: lower bit depths (8- or 16-bit) would truncate the decimal precision of chemical concentration values, introducing systematic errors in the subsequent analysis (Panchenko et al., 2023). All layers are reprojected to WGS84/UTM zone 33N to guarantee metric consistency across datasets (Vaughan et al., 2016).
3. GIS Integration and Spatial Overlay: Within QGIS, raster environmental layers and vector infrastructure data are overlaid. This step enables direct correlation between measured pollution levels, urban morphology, and transport infrastructure, allow-

ing the disaggregation of source contributions across the study area.

4. Hotspot Identification and Decision Support: Thematic maps of maximum concentration areas are produced to identify critical hotspots. From an applied standpoint, these outputs serve a concrete function: guiding local authorities in the placement of future ground-based monitoring stations, so that limited financial resources are directed toward the areas of highest population exposure.

3. Workflow implementation

3.1. Satellite data acquisition and type

For the analysis presented here, the months of February, May, and July 2025 were selected. This choice allows the seasonal variability of emission regimes characterizing the study area to be captured, as the region is strongly influenced by the interaction between climatic dynamics and anthropogenic pressures associated with tourism. February was selected to represent winter baseline conditions, typically characterized by greater atmospheric stability and an additional contribution from residential heating emissions. This period makes it possible to examine the spatial distribution of pollutants in the absence of significant tourist flows. The month of May represents a transition phase, during which the onset of the tourist season becomes evident and solar irradiance progressively increases, factors that directly influence the transformation kinetics of atmospheric pollutants. Finally, July was included to investigate the period of maximum anthropogenic pressure, corresponding to the peak intensity of scheduled maritime transport, cruise ship activity, and vehicular mobility along the main road network of the peninsula. The comparison among these three periods enables the isolation of the impact of anthropogenic precursors under conditions characterized by substantial variability in the atmospheric mixing layer and enhanced photochemical reactivity typical of the Mediterranean basin, thus providing an integrated perspective on air quality conditions across the Sorrentine Peninsula.

The proposed workflow integrates multi-source data to map the main air pollutants and their related anthropogenic pressures. The choice of datasets is guided by the need to ensure continuous spatial coverage in a data-scarcity context, using exclusively open-source resources (Gupta et al., 2006).

- Nitrogen dioxide (NO_2): For NO_2 monitoring, data from the TROPOMI (Tropospheric Monitoring Instrument) sensor aboard ESA's Sentinel-5P mission were used. Although the sensor provides Level 2 (L2) products organized by orbits (swaths) with a native spatial resolution of 3.5×5.5 km, for the purposes of this GIS analysis, monthly means reprocessed from the S5P-PAL portal were acquired, with Level 3 (Eskes et al., 2022; Sentinel-5P Product Algorithm Laboratory [S5P-PAL], n.d.). These data represent the vertical tropospheric column of NO_2 (van Geffen et al., 2020). From a technical point of view, the raw data is stored in NetCDF files using the SI unit of mol/m^2 (moles per square meter). However, to facilitate cartographic interpretation and GIS software management, values were treated as micromoles per square meter (μmol/m^2).
- To preserve the scientific integrity of the data during gridding and clipping, the 32-bit float GeoTIFF format was adopted. This technical choice is crucial: unlike 8- or 16-bit formats, 32-bit float prevents rounding of decimal values, ensuring that micro-variations in concentration are not lost during spatial overlay (Vaughan et al., 2016).
- Fine Particulate Matter ($PM_{2.5}$): Estimated by integrating Aerosol Optical Depth (AOD) data from MODIS sensors and the Copernicus Atmosphere Monitoring Service (CAMS) (Inness et al., 2019).
- Land Use: CORINE Land Cover (CLC) 2018 product from the Copernicus service, with a resolution of 100 m (Büttner, 2014), essential for distinguishing densely urbanized areas from forested or agricultural areas.
- Infrastructure and Transport: Vector data extracted from OpenStreetMap (OSM) (Haklay & Weber, 2008), including the primary road network, port locations, and scheduled shipping routes.

The choice of these datasets, shown in Table 2, is justified by their open-source nature and their ability to provide continuous spatial coverage, overcoming the limitations of point-based stations.

Table 2. Matrix of geospatial datasets and multi-source information layers integrated into the GIS workflow for air quality assessment in the domain under study

Information Layer	Type	Unit of measure	Source / Sensor	Resolution
Tropospheric NO_2	Raster (32-bit float)	μmol/m^2	Sentinel-5P TROPOMI	3.5× 5.5 km
$PM_{2.5}$ (AOD proxy)	Raster (32-bit float)	μg/m^s	MODIS / Copernicus	1 km/ 0.1°
Land Use (CLC)	Raster/ Vector	Land Cover Classes	Copernicus Land Service	100 m
Road Network	Vector (Lines)		Open-StreetMap (OSM)	High (OSM)
Ports and Sea Routes	Vector (Points/ Lines)		OSM	High
Administrative Boundaries	Vector (Poligons)		ISTAT	High

Note: The table analytically describes the technical parameters of the satellite proxies and ancillary data used for spatial pollutant modeling.

3.2. Preporocessing and spatial overlay

Following the preliminary phase of data acquisition and selection, the workflow proceeds with the more technical steps carried out directly within a GIS environment. These include:

- Preprocessing: Rasterization of the satellite data and clipping over the area of interest corresponding to the Sorrentine Peninsula, performed within the GIS environment.
- Spatial Overlay: Superposition of the satellite datasets with critical infrastructures extracted from OpenStreetMap, such as ports and maritime routes, to identify the contribution associated with both road and maritime traffic.
- Hotspot Analysis: Application of buffer analysis and urban density maps (ISTAT/Copernicus datasets) to identify areas characterized by the highest levels of population exposure. These aspects are described in detail in the results section that follows.

For the assessment of tropospheric NO_2 concentrations, monthly averages were obtained through the S5P-PAL portal, based on Level 3 (L3) products derived from the TROPOMI sensor. The GIS processing workflow was designed to preserve the radiometric integrity of the original satellite datasets.

Each dataset was subjected to a spatial clipping procedure, defining an analysis domain encompassing the Sorrentine Peninsula together with part of the Naples metropolitan area. This configuration allows the emission gradient between the dense urban agglomeration and the adjacent coastal sectors to be captured. The cartographic projection was standardized using the EPSG:4326 coordinate reference system. Finally, to ensure strict inter-monthly comparability of the spatial distributions, a normalization of the legends and associated color scales was performed. A common confidence interval was defined, with thresholds ranging between X and Y μmol m^{-2}, applied consistently through a single-band pseudo-color symbology. This methodological choice removes potential visual biases arising from different data ranges across the seasonal datasets, thereby enabling a coherent and direct evaluation of temporal trends and pollutant dispersion patterns between February, May, and July 2025.

For the estimation of fine particulate matter ($PM_{2.5}$), the dataset "CAMS European Air Quality Analysis" provided by the Copernicus service was employed. This product has a spatial resolution of 0.1°×0.1° (approximately 10 km). The use of this dataset helps overcome the spatial limitations typical of global-scale models, offering a more detailed representation of pollutant dispersion in geographically complex areas such as the Sorrentine Peninsula, where orography and coastal dynamics play a significant role in shaping local air quality patterns. As a result, the dataset provides a representation that is more consistent with the local emission dynamics characterizing the study area. The parameter "Surface Level" (Single Level) was selected in order to focus on pollutant concentrations at ground level. This choice allows the analysis to directly address human exposure near the surface, ensuring consistency with sensitive receptors and anthropogenic infrastructures previously mapped within the GIS framework. The dataset was retrieved with hourly temporal resolution (24-time steps per day) for the entire study period. Temporal aggregation was subsequently performed by calculating the arithmetic mean of all hourly time steps, using the "Cell Statistics" tool with the statistical option set to Mean.

This procedure produces a representation of monthly mean $PM_{2.5}$ concentrations that is not influenced by short-term diurnal fluctuations. Compared with approaches based on instantaneous sampling, this method provides a more statistically robust estimate of pollutant levels and ensures consistency between the modelled data and the monthly averages derived from TROPOMI satellite products.

The GIS workflow was integrated with high-resolution ancillary datasets to support the spatial interpretation of atmospheric variables and to better identify localized and transport-related emission sources within the study domain.

Land-cover information was obtained from the CORINE Land Cover (CLC) 2018 dataset (spatial resolution 100 m), which enables the discrimination of urbanized areas from agricultural and natural surfaces. This layer was used as a reference to contextualize the spatial distribution of pollutant concentrations in relation to the underlying surface characteristics.

As with the $PM_{2.5}$ data, the CORINE dataset was downloaded through Copernicus services and can be readily used within common GIS software environments such as QGIS. To better account for transport-related emission processes, vector layers were retrieved from OpenStreetMap (OSM) through the web services available within the GIS platform.

Bringing these datasets together makes it possible to examine how the spatial patterns of NO_2 and $PM_{2.5}$ concentrations relate to the main mobility corridors of the region. In particular, it allows the pollutant fields to be interpreted in relation to major road axes, scheduled maritime connections, and cruise ship traffic, thereby offering a clearer picture of the anthropogenic factors that contribute to shaping air quality conditions across the study area.

4. Results and discussion

4.1. NO_2 mapping

The analysis was performed on a 3.5×5.5 km grid, allowing the identification of large-scale spatial trends and seasonal mean patterns. In addition, all datasets were normalized using the same colour scale, ensuring direct

visual comparability between the different periods. The following maps present the NO_2 concentration fields for the three months considered in the analysis.

Figure 4 shows the spatial distribution of the monthly mean tropospheric column concentration of nitrogen dioxide (NO_2) for February 2025. The data, derived from the TROPOMI sensor (Sentinel-5P) and processed through the S5P-PAL portal, are expressed in μmol m^{-2}. The map highlights a pronounced northwest–southeast gradient, with the primary hotspot located over the Naples metropolitan area (maximum values of approximately 158 μmol m^{-2}) and a progressive decrease in concentrations along the Sorrentine Peninsula ridge. The red boundaries indicate the municipal administrative limits within the study domain. The spatial resolution of the reprojected dataset allows the different emission signatures of the urbanized coastal sectors and the mountainous areas of the Lattari Mountains to be distinguished, where minimum values of approximately 20 μmol m^{-2} are observed. In Figure 5 it can be seen the spatial distribution of the monthly mean tropospheric column concentration of nitrogen dioxide (NO_2) for May 2025. The map shows a marked reduction in average concentrations across the entire domain compared with the winter period. The disappearance of the urban hotspot over Naples and the shift toward lower-value color tones indicate the seasonal increase in solar radiation and temperature, which enhance the photolysis processes affecting NO_2. Figure 6 shows the spatial distribution of the monthly mean tropospheric column concentration of nitrogen dioxide (NO_2) for July 2025. Despite normalization using the same reference color scale, the map confirms the lowest values of the year, associated with the peak intensity of summer photochemical dissociation processes. A weak but persistent signal (light green tones) can still be observed over the Gulf of Naples and along the main navigation corridors of the Sorrentine Peninsula. Although the overall tropospheric column is relatively depleted, this spatial pattern suggests the continued influence of maritime and cruise ship emissions, which typically reach their maximum operational frequency in July, partially offsetting the otherwise strong photochemical removal of NO_2.

The figures below illustrate selected examples of the GIS overlay performed using the different informational layers incorporated into the analysis. Specifically, Figure 7 represents the proximity analysis between tropospheric column NO_2 concentrations (TROPOMI) and transport infrastructures in the Sorrentine Peninsula, July 2025. The map combines the normalized satellite data with vector layers representing the road network (OSM Traffic) and maritime routes (OSM Tracks). Despite the seasonal minimum of gaseous pollutants associated with enhanced summer photolysis, a persistent signal can still be observed along the SS145 road corridor and across the Naples–Sorrento–Capri maritime routes. Finally, Figure 8 depicts the integrated analysis of NO_2 concentrations (February 2025), transport infrastructures, and land-use classes derived from CORINE Land Cover. The overlay reveals a clear spatial association

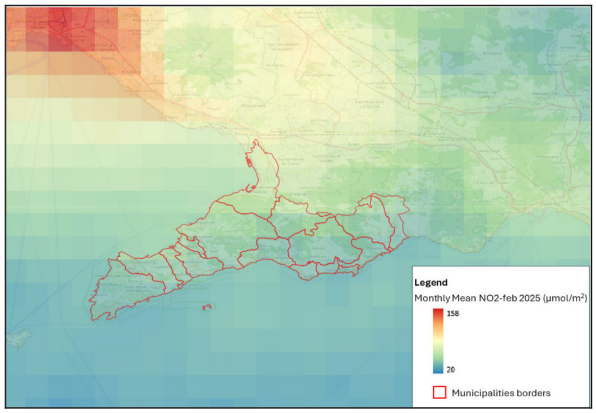

Figure 4. Spatial distribution of the monthly mean tropospheric column concentration of nitrogen dioxide (NO_2) for February 2025. Data derived from the TROPOMI sensor (Sentinel-5P) and processed through the S5P-PAL portal, expressed in μmol m^{-2}

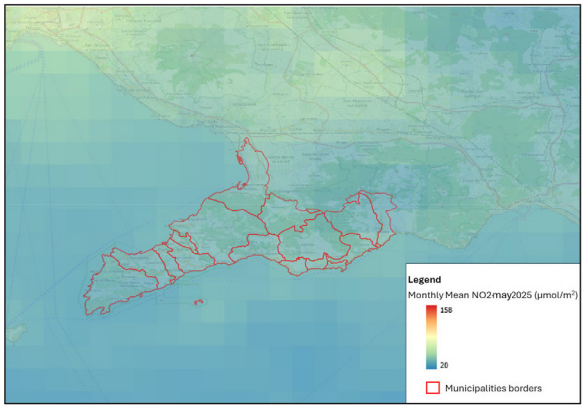

Figure 5. Spatial distribution of the monthly mean tropospheric column concentration of nitrogen dioxide (NO_2) for May 2025

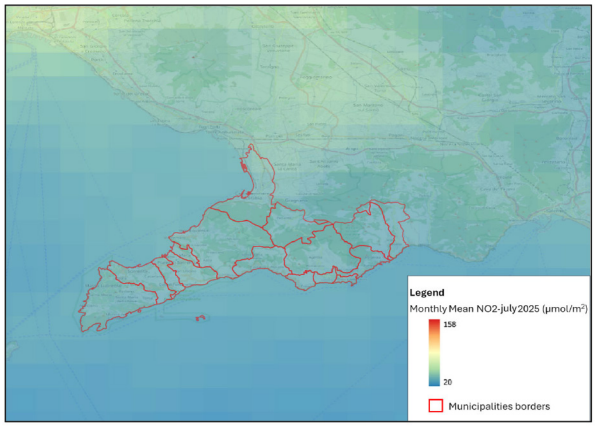

Figure 6. Spatial distribution of the monthly mean tropospheric column concentration of nitrogen dioxide (NO_2) for July 2025

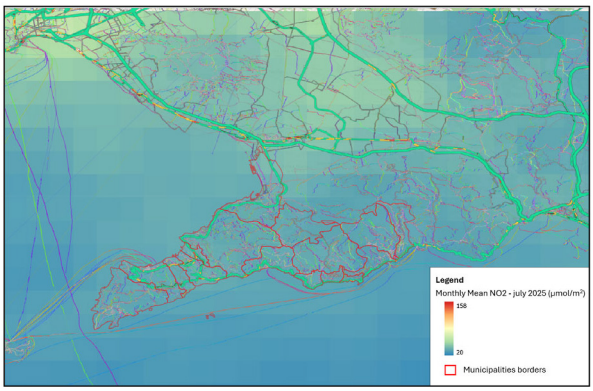

Figure 7. Proximity analysis between tropospheric column NO_2 concentrations (TROPOMI) and transport infrastructures in the Sorrentine Peninsula, July 2025

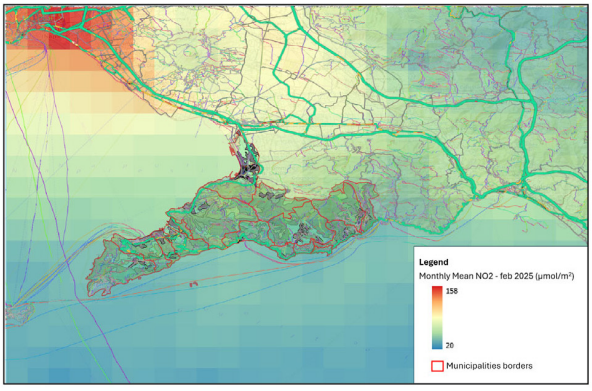

Figure 8. Integrated analysis of NO_2 concentrations (February 2025), transport infrastructures, and land-use classes derived from CORINE Land Cover

between the highest NO_2 levels and areas categorized as continuous or discontinuous urban fabric and industrial/commercial zones (displayed in dark grey and black in the map).

4.2. $PM_{2.5}$ mapping

In Figure 9 it is shown the Spatial distribution of the monthly mean surface concentration of fine particulate matter ($PM_{2.5}$) for February 2025. The data are derived from the CAMS European Air Quality high-resolution analysis (0.1°) and are expressed in µg m^{-3}. The map highlights a marked accumulation of particulate matter across the inland areas of the Naples basin, particularly within the Nola–Sarno plain, where maximum values reach approximately 59 µg m^{-3}. These elevated concentrations are consistent with wintertime thermal inversion conditions and the associated accumulation of combustion- and traffic-related particulate emissions. Figure 10 shows the Spatial distribution of the monthly mean surface concentration of $PM_{2.5}$ for May 2025. The data are normalized using the winter reference scale (5–59 µg m^{-3}). The map shows a general decrease in concentrations compared with the winter period. However, the Sorrentine Peninsula exhibits a persistence of intermediate values (green–yellow tones, approximately 25–30 µg m^{-3}), comparable to those observed in the Naples hinterland. This relatively uniform spatial pattern suggests that, despite the marked reduction in heating-related emissions over Naples, the Sorrentine Peninsula maintains a persistent background level of particulate matter. Such conditions may reflect the combined influence of seasonally increasing vehicular traffic linked to tourism and the contribution of marine aerosols, which can contribute to maintaining stable $PM_{2.5}$ concentrations in coastal environments even during periods characterized by enhanced atmospheric mixing. Finally in Figure 11 is reported the Spatial distribution of the monthly mean surface concentration of $PM_{2.5}$ for July 2025. The data are normalized using the reference scale (5–59 µg m^{-3}). The map highlights the lowest concentrations observed during the entire study period across most of the domain, with the Sorrentine Peninsula displaying relatively homogeneous blue tones corresponding to values of approximately 10–15 µg m^{-3}. This pattern reflects typical summer atmospheric conditions, characterized by increased instability and the absence of emissions associated with residential heating.

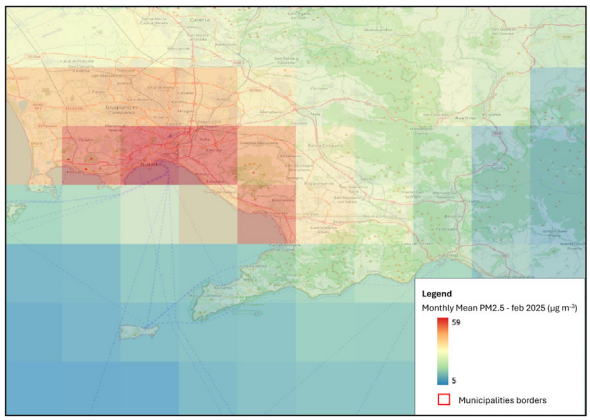

Figure 9. Spatial distribution of the monthly mean surface concentration of fine particulate matter ($PM_{2.5}$) for February 2025

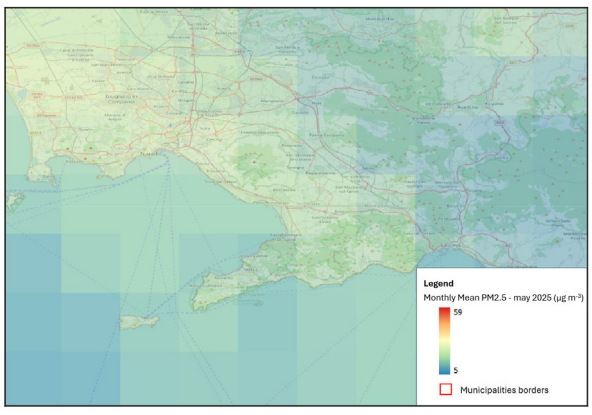

Figure 10. Spatial distribution of the monthly mean surface concentration of $PM_{2.5}$ for May 2025

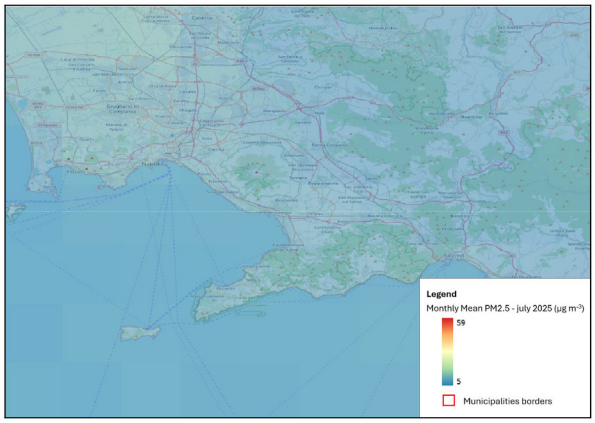

Figure 11. Spatial distribution of the monthly mean surface concentration of $PM_{2.5}$ for July 2025

Nevertheless, the presence of slight gradients along the coastline and near the main port areas indicates that emissions related to maritime traffic and seasonal road mobility still exert a localized influence. These contributions, although reaching their seasonal maximum during summer, appear to be effectively dispersed by coastal breeze circulations and enhanced vertical mixing within the atmospheric boundary layer.

A more detailed examination of the NO_2 signal reveals a pattern that diverges from what would be expected based solely on anthropogenic emission fluxes. Although tourism-related mobility and maritime traffic reach their seasonal maximum in July, the NO_2 tropospheric column measured by TROPOMI is lower than in winter, with values around 34 µmol m^{-2} in July compared to approximately 52 µmol m^{-2} in February. This behaviour highlights the dominant role of atmospheric photolysis and the dilution associated with the seasonal deepening of the atmospheric mixing layer (Ding et al., 2020).

The pronounced peak observed over Naples in February (approximately 158 µmol m^{-2}) appears instead to be linked to the accumulation of pollutants under stable atmospheric conditions, particularly thermal inversions, which favour the trapping of emissions within the lower troposphere. These findings indicate that, in coastal environments, meteorological forcing and atmospheric chemistry may exert a stronger control on pollutant concentrations than the simple variability of emission sources (Lorente et al., 2019). Nitrogen dioxide is a molecule highly sensitive to ultraviolet radiation. During July, the intense Mediterranean solar irradiance enhances the photochemical cycle: $NO_2 + h\nu \rightarrow NO + O$.

This reaction proceeds significantly faster in summer than in winter, drastically reducing the atmospheric lifetime of NO_2. As a result, even though emissions from ferries, cruise ships, and seasonal road traffic increase during the summer months, the rapid photochemical removal of NO_2 leads to lower monthly mean values detected by the satellite observations.

As illustrated in Figure 7, the integration of OpenStreetMap (OSM) vector datasets with the July 2025 satellite products allowed a proximity-based spatial analysis aimed at isolating the contribution of transport-related emissions to local air quality. Despite the rapid photochemical removal typical of the summer regime, the cartographic overlay reveals a consistent spatial correspondence between relative NO_2 enhancements and the main road and maritime transport corridors (Georgoulias et al., 2020). A closer inspection of the Sorrentine Peninsula highlights a clear spatial alignment between positive anomalies in the NO_2 signal (green–yellow tonalities) and the trajectory of the SS145 Sorrentina road corridor. The strengthening of the signal near port interchange nodes suggests that seasonal anthropogenic pressure, although subject to strong dilution due to convective mixing and reduced atmospheric stability, still produces a persistent emission footprint spatially constrained to key transport infrastructures. Particularly relevant is the inclusion of maritime trajectories (OSM tracks), whose analysis underlines the emissive relevance of high-speed passenger vessels (hydrofoils and ferries) as well as cruise ship traffic. The persistence of the NO_2 signal along the maritime connections linking Naples, Sorrento, and Capri represents a notable scientific observation. Under summer conditions, when the atmosphere is thermally unstable and largely free from stationary terrestrial emission sources such as residential heating, the contribution from mobile maritime sources becomes proportionally more significant. In this context, shipping traffic acts as a continuous mobile source, capable of influencing the tropospheric column above the marine boundary layer and shaping the air quality profile along the entire coastal sector of the study domain (Ding et al., 2020).

In Figure 8, which depicts the February NO_2 distribution, the main terrestrial and maritime transport corridors were overlaid together with CORINE Land Cover classes, where the principal urban settlements are highlighted in darker grey and black tones. The land-use representation allows the contribution of anthropogenic heating emissions during winter to be clearly appreciated. The areas showing higher NO_2 levels (yellowish colours) correspond closely to urban centres and the metropolitan core of Naples, confirming the strong spatial relationship between emission maxima and areas classified as "continuous and discontinuous urban fabric" (CLC classes 111 and 112) and "industrial or commercial units" (CLC class 121) (Cersosimo et al., 2020). A progressive decrease in pollutant levels can be observed toward the forested and semi-natural areas of the Lattari Mountains ridge (CLC classes 311 and 321), where the signal weakens significantly. This gradient further confirms the capability of TROPOMI satellite observations to discriminate between active anthropogenic emission sources and areas characterized by background atmospheric conditions or natural sinks. With regard to $PM_{2.5}$, the comparative analysis of the raster products

for February, May, and July 2025 reveals a pronounced seasonal variability, governed by the interaction between anthropogenic forcing, meteorological regimes, and local thermodynamic conditions. In February, the signal reaches its highest levels (up to 59 μg m^{-3}), with critical hotspots located over the Naples metropolitan area and the Nola–Sarno inland basin. Although the Sorrentine Peninsula shows slightly lower values, concentrations remain moderately elevated, likely due to the combined effect of residential heating emissions (including biomass combustion) and stable atmospheric conditions. During this period, frequent surface thermal inversions, the absence of persistent sea-breeze circulation, and the dominance of high-pressure systems reduce the thickness of the mixing layer, favouring pollutant accumulation. In addition, the Lattari Mountains orography acts as a partial barrier to horizontal dispersion, promoting the advective transport of pollutants along the coastal sector (Garrido-Perez et al., 2018). The transition to May (Figure 10) shows a shift toward a more homogeneous spatial distribution. The marked reduction of concentrations in the urban area (from approximately 59 μg m^{-3} to 23 μg m^{-3}) reflects the cessation of residential heating activities. Nevertheless, the persistence of a relatively constant background concentration over the Sorrentine Peninsula (25–30 μg m^{-3}) values comparable to those observed in the urban core is noteworthy. This spatial uniformity suggests that, under springtime conditions, $PM_{2.5}$ behaves increasingly as a regional-scale pollutant, influenced both by secondary aerosol formation processes and by the increase in vehicular traffic associated with the onset of the tourist season (Guth et al., 2018). Finally, July (Figure 11) displays the lowest $PM_{2.5}$ concentrations of the entire study period, despite the seasonal maximum in anthropogenic pressure and maritime mobility. This apparently paradoxical behaviour can be explained by the efficient dispersion mechanisms typical of the Mediterranean summer regime. Strong solar heating induces sea-breeze circulation during daytime and land-breeze flows at night, generating a persistent ventilation regime often exceeding 5–8 m s^{-1}, which promotes the dilution and vertical redistribution of particulate matter.

The weak residual gradients observed near port infrastructures and along the peninsula's main transport corridors indicate the influence of local emission sources, particularly shipping and road traffic. However, despite operating at their seasonal peak, these sources remain subject to an atmospheric environment characterized by substantially greater dispersive capacity than during the winter semester.

5. Conclusions

The combined use of geoinformation and remote sensing techniques provides a cost-effective and operationally efficient framework for the early identification of air-quality hotspots. GIS-based systems enable the management and analysis of large spatial datasets over extended domains with high computational efficiency, while also facilitating continuous updates of the underlying data layers and analytical models. The proposed workflow offers several methodological advantages, as follows.

- Centralized data management: Geographic information is organized within a unified relational database environment (DBMS), allowing consistent storage and access to heterogeneous spatial datasets.
- Data integrity: The database structure preserves spatial consistency and reduces the risk of discrepancies among the different geospatial layers used in the analysis.
- Decision-support capability: The framework enables rapid identification of priority areas where future in situ monitoring campaigns may be required by environmental agencies.
- Replicability: The reliance on open-source datasets and tools makes the methodology transferable to different geographical contexts and fully implementable within a standard GIS environment.
- Multilayer and multidisciplinary integration: Air-quality observations, meteorological variables, and dispersion-model outputs can be integrated within a unified all-in-one analytical system, allowing cross-disciplinary analyses.
- Operational accessibility: The system remains relatively straightforward to operate, enabling its use not only by technical personnel but also by policy makers and environmental managers, with potential applications in early-warning and environmental management frameworks.

The spatiotemporal analysis for 2025 reveals a strong seasonal decoupling between emission sources and observed concentrations. During the analyzed period, NO_2 peaked in February at 158 μmol m^{-2} (Naples hotspot) but declined to 34 μmol m^{-2} in July, due to intense summer photolysis despite increased maritime and tourist traffic. Similarly, $PM_{2.5}$ decreased from winter highs of 59 μg m^{-3} to summer lows of 10–15 μg m^{-3}, as enhanced vertical mixing and sea breeze circulation effectively disperse anthropogenic loads. Ultimately, the results demonstrate that meteorological forcing and photochemical rates exert a dominant control on air quality levels in the Sorrento Peninsula, prevailing over seasonal fluctuations in transport-related emissions.

Overall, the adoption of object-oriented spatial data models allows infrastructures, emission sources, and pollutants to be treated as interconnected entities within the same geospatial framework. This structure provides a robust basis for addressing complex geoinformatics problems and represents a practical decision-support tool for environmental monitoring agencies. At the same time, the approach highlights several technical limitations and areas for further development. The spatial resolution adopted in this study largely constrained by the characteristics of the input datasets may lead to an

underestimation of localized concentration peaks, particularly within narrow valleys and complex orographic environments. For applications oriented toward Environmental Impact Assessment, a more rigorous validation would likely require the integration of ground-based measurements, such as those provided by the ARPAC monitoring network, in order to verify and calibrate the satellite derived products. Paradoxically, however, it is precisely in contexts where monitoring networks are sparse that approaches of this type become most valuable.

Another limitation arises from the heterogeneity of the datasets employed, which differ in both spatial and temporal resolution. Future developments may therefore benefit from the implementation of interpolation and resampling techniques, potentially through dedicated GIS plugins, in order to harmonize the datasets within a consistent spatial and temporal framework. These aspects also highlight the inherently multidisciplinary nature of air-quality data analysis, which requires the integration of atmospheric science, geoinformatics, and environmental monitoring methodologies. Future developments of the workflow aim to move beyond a purely descriptive mapping approach toward a framework capable of quantitatively supporting strategic monitoring planning. The integration of high-resolution dispersion models would enable the estimation of pollutant concentrations at neighbourhood or district scale, significantly improving the spatial detail of exposure assessments. Such spatial resolution is essential for translating environmental datasets into population exposure indicators, enabling not only environmental analyses but also targeted epidemiological investigations that explore potential correlations between pollution hotspots and the incidence of respiratory and cardiovascular diseases.

Within this perspective, the GIS system can function as a decision-support platform for both environmental and public-health authorities, assisting in the design of coherent, multidisciplinary, and multiparametric monitoring networks. This includes the potential deployment of low-cost sensor stations distributed over wide spatial areas, improving coverage in regions characterized by complex topography and heterogeneous climatic regimes. Ultimately, this integrated approach provides the knowledge base required for the development of health-oriented air-quality management strategies, aimed at mitigating pollutant exposure in the most vulnerable and densely populated areas.

References

Bechle, M. J., Millet, D. B., & Marshall, J. D. (2013). Remote sensing of exposure to NO_2: Satellite versus ground-based measurement in a large urban area. *Atmospheric Environment*, *69*, 345–353. https://doi.org/10.1016/j.atmosenv.2012.11.046

Büttner, G. (2014). CORINE land cover and land cover change products. In I. Manakos & M. Braun (Eds.), *Remote sensing and digital image processing*: *Vol. 18. Land use and land cover mapping in Europe*: *Practices* & *trends* (pp. 55–74). Springer. https://doi.org/10.1007/978-94-007-7969-3_5

Cersosimo, A., Serio, C., & Masiello, G. (2020). TROPOMI NO_2 tropospheric column data: Regridding to 1 km grid-resolution and assessment of their consistency with in situ surface observations. *Remote Sensing*, *12*(14), Article 2212. https://doi.org/10.3390/rs12142212

Cohen, A. J., Brauer, M., Burnett, R., Anderson, H. R., Frostad, J., Estep, K., Balakrishnan, K., Brunekreef, B., Dandona, L., Dandona, R., Feigin, V., Freedman, G., Hubbell, B., Jobling, A., Kan, H., Knibbs, L., Liu, Y., Martin, R., Morawska, L., … Forouzanfar, M. H. (2017). Estimates and 25-year trends of the global burden of disease attributable to ambient air pollution: An analysis of data from the Global Burden of Diseases Study 2015. *The Lancet*, *389*(10082), 1907–1918. https://doi.org/10.1016/S0140-6736(17)30505-6

Contini, D., Gambaro, A., Belosi, F., De Pieri, S., Cairns, W. R. L., Donateo, A., Zanotto, E., & Citron, M. (2011). The direct influence of ship traffic on atmospheric $PM_{2.5}$, PM_{10} and PAH in Venice. *Journal of Environmental Management*, *92*(9), 2119–2129. https://doi.org/10.1016/j.jenvman.2011.01.016

Copernicus Sentinel-5P. (2021). *TROPOMI Level 2 Nitrogen Dioxide total column products* (Version 02) [Dataset]. European Space Agency. https://doi.org/10.5270/S5P-9bnp8q8

de Hoogh, K., Chen, J., Gulliver, J., Hoffmann, B., Hertel, O., Ketzel, M., Bauwelinck, M., van Donkelaar, A., Hvidtfeldt, U. A., Katsouyanni, K., Klompmaker, J., Martin, R. V., Samoli, E., Schwartz, P. E., Stafoggia, M., Bellander, T., Strak, M., Wolf, K., Vienneau, D., & Hoek, G. (2018). Spatial $PM_{2.5}$, NO_2, O_3 and BC models for Western Europe – Evaluation of spatiotemporal stability. *Environment International*, *120*, 81–92. https://doi.org/10.1016/j.envint.2018.07.036

Ding, J., van der A, R. J., Eskes, H. J., Mijling, B., Stavrakou, T., Van Geffen, J. H. G. M., & Veefkind, J. P. (2020). NOx emissions reduction and rebound in China due to the COVID-19 crisis. *Geophysical Research Letters*, *47*(19), Article e2020GL089912. https://doi.org/10.1029/2020GL089912

Eskes, H., van Geffen, J., Boersma, F., Eichmann, K.-U., Apituley, A., Pedergnana, M., Sneep, M., Veefkind, P. J., & Loyola, D. (2022). *Sentinel-5 precursor/TROPOMI Level 2 product user manual nitrogen dioxide* (Issue 4.1.0, Report No. S5P-KNMI-L2-0021-MA). Royal Netherlands Meteorological Institute (KNMI). https://sentinels.copernicus.eu/documents/247904/2474726/Sentinel-5P-Level-2-Product-User-Manual-Nitrogen-Dioxide.pdf

European Environment Agency. (2023). *Air quality in Europe 2023* (EEA Report No. 01/2023). https://doi.org/10.2800/7636500

Garrido-Perez, J. M., Ordóñez, C., García-Herrera, R., & Barriopedro, D. (2018). Air stagnation in Europe: Spatiotemporal variability and impact on air quality. *Science of the Total Environment*, *645*, 1238–1252. https://doi.org/10.1016/j.scitotenv.2018.07.238

Georgoulias, A. K., Boersma, K. F., Van Vliet, J., Zhang, X., Van Der A, R., Zanis, P., & De Laat, J. (2020). Detection of NO_2 pollution plumes from individual ships with the TROPOMI/S5P satellite sensor. *Environmental Research Letters*, *15*(12), Article 124037. https://doi.org/10.1088/1748-9326/abc445

Giovannini, L., Ferrero, E., Karl, T., Rotach, M. W., Staquet, C., Trini Castelli, S., & Zardi, D. (2020). Atmospheric pollutant dispersion over complex terrain: Challenges and needs for improving air quality measurements and modeling. *Atmosphere*, *11*(6), Article 646. https://doi.org/10.3390/atmos11060646

Guevara, M., Jorba, O., Soret, A., Petetin, H., Bowdalo, D., Serradell, K., Tena, C., Denier van der Gon, H., Kuenen, J., Peuch, V.-H., & Pérez García-Pando, C. (2021). Copernicus Atmosphere Monitoring Service TEMPOral profiles (CAMS-TEMPO): Global and European emission temporal profile maps for atmospheric chemistry modelling. *Earth System Science Data*, *13*(2), 367–404. https://doi.org/10.5194/essd-13-367-2021

Gupta, P., Christopher, S. A., Wang, J., Gehrig, R., Lee, Y. C., & Kumar, N. (2006). Satellite remote sensing of particulate matter and air quality assessment over global cities. *Atmospheric Environment*, *40*(30), 5880–5892. https://doi.org/10.1016/j.atmosenv.2006.03.016

Guth, J., Marécal, V., Josse, B., Arteta, J., & Hamer, P. (2018). Primary aerosol and secondary inorganic aerosol budget over the Mediterranean Basin during 2012 and 2013. *Atmospheric Chemistry and Physics*, *18*(7), 4911–4934. https://doi.org/10.5194/acp-18-4911-2018

Haklay, M., & Weber, P. (2008). Openstreetmap: User-generated street maps. *IEEE Pervasive Computing*, *7*(4), 12–18. https://doi.org/10.1109/MPRV.2008.80

Inness, A., Ades, M., Agustí-Panareda, A., Barré, J., Benedictow, A., Blechschmidt, A.-M., Dominguez, J. J., Engelen, R., Eskes, H., Flemming, J., Huijnen, V., Jones, L., Kipling, Z., Massart, S., Parrington, M., Peuch, V.-H., Razinger, M., Remy, S., Schulz, M., & Suttie, M. (2019). The CAMS reanalysis of atmospheric composition. *Atmospheric Chemistry and Physics*, *19*(6), 3515–3556. https://doi.org/10.5194/acp-19-3515-2019

Lelieveld, J., Evans, J. S., Fnais, M., Giannadaki, D., & Pozzer, A. (2015). The contribution of outdoor air pollution sources to premature mortality on a global scale. *Nature*, *525*(7569), 367–371. https://doi.org/10.1038/nature15371

Lorente, A., Boersma, K. F., Eskes, H. J., Veefkind, J. P., van Geffen, J. H. G. M., de Zeeuw, M. B., Denier van der Gon, H. A. C., Beirle, S., & Krol, M. C. (2019). Quantification of nitrogen oxides emissions from build-up of pollution over Paris with TROPOMI. *Scientific Reports*, *9*(1), Article 20033. https://doi.org/10.1038/s41598-019-56428-5

Murena, F., Mocerino, L., Quaranta, F., & Toscano, D. (2018). Impact on air quality of cruise ship emissions in Naples, Italy. *Atmospheric Environment*, *187*, 70–83. https://doi.org/10.1016/j.atmosenv.2018.05.056

Panchenko, S., Ugnenko, I., Yurchenko, V., Uzhviieva, E., Korostelov, Y., & Sorochuk, N. (2023). Innovative methods of using laser scanning and geoinformation systems for design of communication routes. In *12th International Conference "Environmental Engineering"* (pp. 1–4). Vilnius Gediminas Technical University. https://doi.org/10.3846/enviro.2023.843

Sentinel-5P Product Algorithm Laboratory. (n.d.). *Copernicus Sentinel-5P Mapping Portal – Tropospheric NO_2 monthly maps*. S&T Netherlands / European Space Agency. https://maps.s5p-pal.com/no2-tropospheric/month

Sorek-Hamer, M., Chatfield, R., & Liu, Y. (2020). Review: Strategies for using satellite-based products in modeling $PM_{2.5}$ and short-term pollution episodes. *Environment International*, *144*, Article 106057. https://doi.org/10.1016/j.envint.2020.106057

Van Donkelaar, A., Martin, R. V., Brauer, M., Hsu, N. C., Kahn, R. A., Levy, R. C., Lyapustin, A., Sayer, A. M., & Winker, D. M. (2016). Global estimates of fine particulate matter using a combined geophysical-statistical method with information from satellites, models, and monitors. *Environmental Science & Technology*, *50*(7), 3762–3772. https://doi.org/10.1021/acs.est.5b05833

Van Geffen, J., Boersma, K. F., Eskes, H., Sneep, M., Ter Linden, M., Zara, M., & Veefkind, J. P. (2020). S5P TROPOMI NO_2 slant column retrieval: Method, stability, uncertainties and comparisons with OMI. *Atmospheric Measurement Techniques*, *13*(3), 1315–1335. https://doi.org/10.5194/amt-13-1315-2020

Vaughan, A. R., Lee, J. D., Misztal, P. K., Metzger, S., Shaw, M. D., Lewis, A. C., Purvis, R. M., Carslaw, D. C., Goldstein, A. H., Hewitt, C. N., Davison, B., Beevers, S. D., & Karl, T. G. (2016). Spatially resolved flux measurements of NO_x from London suggest significantly higher emissions than predicted by inventories. *Faraday Discussions*, *189*, 455–472. https://doi.org/10.1039/C5FD00170F

Veefkind, J. P., Aben, I., McMullan, K., Förster, H., de Vries, J., Otter, G., Claas, J., Eskes, H. J., de Haan, J. F., Kleipool, Q., van Weele, M., Hasekamp, O., Hoogeveen, R., Landgraf, J., Snel, R., Tol, P., Ingmann, P., Voors, R., Kruizinga, B., … Levelt, P. F. (2012). TROPOMI on the ESA Sentinel-5 Precursor: A GMES mission for global observations of the atmospheric composition for climate, air quality and ozone layer applications. *Remote Sensing of Environment*, *120*, 70–83. https://doi.org/10.1016/j.rse.2011.09.027

World Health Organization. (2021). *WHO global air quality guidelines: Particulate matter ($PM_{2.5}$ and PM_{10}), ozone, nitrogen dioxide, sulfur dioxide and carbon monoxide*. https://www.who.int/publications/i/item/9789240034228